SOILS AND FOUNDATIONS Vol. 16, No. 1, Mar. 1976
Japanese Society of Soil Mechanics and Foundation Engineering

LOCAL STRAINS AND DISPLACEMENT PATTERNS IN TRIAXIAL SPECIMENS OF A SATURATED CLAY

A. S. BALASUBRAMANIAM*

ABSTRACT

An X-ray technique is used for the determination of local strains in triaxial specimen of saturated Kaolin during shear under stress-controlled conditions. The axial and radial strain distributions in 1.5 in. diameter by 3.0 in. high samples contained between friction ends and lubricated ends are presented. The principal axes of local strains are found to coincide with the vertical and horizontal axes of the specimen. The overall axial and volumetric strains computed from the local strain measurements are in excellent agreement with the overall average measurements conventionally measured using a dial gauge and a burette. During progressive failure in compression rigid zones were found to develop at the two ends of the specimen. No rigid zones were observed during progressive failure in extension tests.

Key words: progressive failure, strain, triaxial compression test
IGC: D0/D6

INTRODUCTION

The non-uniform deformation of soil specimens during shear has been considered by most research workers to be the largest source of error in the experimental study of the stress-strain relationships of soils. Theoretical investigation of the distribution of stresses and strains in cylindrical specimens under compression and in extension have been carried out by Filon (1902), Pickett (1944), D'Appolonia and Newmark (1951), Balla (1960) and other research workers. The theoretical methods developed by all these workers are only applicable to elastic media. The deformation of clay specimens are mainly plastic and hence these methods have only limited applications in soil mechanics problems. Besides the theoretical studies carried out by the above authors, experimental evidence confirming the non-uniformity of deformation in triaxial specimens was cited by a number of authors, notably Geuze and Tan (1950), Rowe and Barden (1964) who worked with saturated clay samples and Shockley and Ahlvin (1960) who worked with sand samples. The method adopted by these authors and others was to determine the moisture content of portions of clay and frozen sand cut from the test specimens. This procedure takes time and the moisture content can only be determined at the end of the test. In contrast to this procedure Roscoe, Schofield and Thurairajah (1963) described a method of measuring the local variations of strains throughout a triaxial sample both in compression and in extension. In this method a number of horizontal lines had been painted on the membrane of the triaxial sample. The height and diameter of each element was measured by means of a

* Associate Professor, Division of Geotechnical Engineering, Asian Institute of Technology, Bangkok, Thailand.
Written discussions on this paper should be submitted before January 1, 1977.

theodolite and the corresponding axial and radial strains were determined. While this method was far from precise, it gave an overall idea of the local strains and voids ratio in the triaxial specimens. Accurate measurements were limited by the assumptions namely (i) each element deformed uniformly within itself (ii) the reference lines defining the boundaries of the element were circular in horizontal planes throughout the testing, (iii) no soil passed from one element to another during the deformation of the soil and (iv) the volume of an element was determined by assuming that it was a truncated cone. X-ray technique was first used by Roscoe, Arthur and James (1963 a, b) for the measurement of strains in sand. Sirwan (1965) studied the local variations of strains and voids ratio in triaxial sand specimens using (i) the lead shot technique and (ii) the X-ray absorption method with film density measurements. The local strains during one dimensional consolidation, using X-ray and the lead-shot technique were carried out by Burland and Roscoe (1970).

Most of the experimental work mentioned above was carried out on sand samples. Very little progress has been made in the study of local strains in clay specimens. The present paper is concerned with a detailed investigation (using the X-ray lead shot technique) of the distributions of strains in normally and overconsolidated clay specimens both in compression and in extension.

DEFINITION OF STRESS AND STRAIN PARAMETERS

The stress parameters used in the analysis of the triaxial test results are

$$p=(\sigma_1'+2\sigma_3')/3$$

and

$$q=(\sigma_1'-\sigma_3') \quad \text{since } \sigma_2'=\sigma_3'$$

where σ_1', σ_2', and σ_3' are the principal effective compressive stresses. In terms of the principal compressive strains ε_1, ε_2 and ε_3, the relevant strain parameters for use under the axisymmetric conditions of the triaxial test are

$$v=\varepsilon_1+2\varepsilon_3$$

and

$$\varepsilon=\frac{2}{3}(\varepsilon_1-\varepsilon_3) \quad \text{since } \varepsilon_2=\varepsilon_3$$

The parameter $\eta=q/p$. For detailed descriptions of these parameters reference could be made to Roscoe, Schofield and Wroth (1958), Schofield and Wroth (1968).

MATERIAL TESTED, SAMPLE PREPARATION AND TESTING PROCEDURE

All specimens were prepared from air-dried Kaolin (liquid limit 74%, plastic limit 42%, and specific gravity 2.61) mixed with water to a slurry of 160% moisture content. The slurry was one dimensionally consolidated in a special former to a maximum pressure of 22.6 lb/in^2. Subsequently, the former was removed and the sample was isotropically consolidated to the required cell pressure. For a detailed description of the sample preparation and testing procedure (also of the equipment used for X-ray testing, the exposure of X-ray films and processing of exposed X-ray films) see Balasubramaniam (1974). The arrangement of lead markers inside a 1.5 inch diameter by 3.0 inch high sample is shown in Fig. 1. The lead markers were arranged in two mutually perpendicular planes passing through the axis of the sample. Photo 1 illustrates the arrangement of lead markers in a 4 inch diameter sample, on a vertical plane passing through the vertical axis of the sample. However, the number of rows in the orthogonal plane were increased for the 4 inch diameter sample.

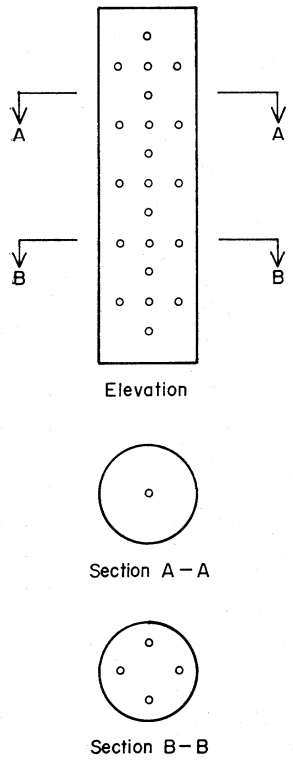

Fig. 1. Arrangement of lead markers in 1.5 inch diameter sample

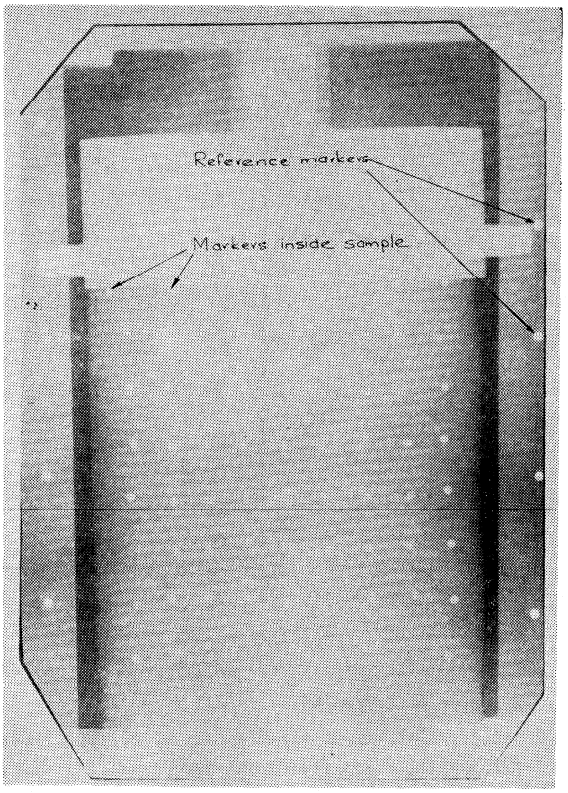

Photo 1. Arrangement of lead markers in 4 inch diameter sample

TEST RESULTS

Effect of End Restraint on the Strains of 1.5 in. Diameter Sample During Shear in Compression Tests

Two types of end conditions were used; (i) The conventional rough end was a 1.5 inch diameter porous stone (3/16 inch thick, type UNI 150 kv) at the base. (ii) Lubricated ends were provided by replacing this porous stone by a 3/16 inch highly polished brass disc covered with a thin layer of silicone grease. Drainage was permitted through a 1/4 inch diameter porosint (Grade B) stud recessed at the centre of this brass disc. In all tests in the triaxial cell with the lubricated ends the top cap was of duralumin with a highly polished lower face covered with a thin layer of silicone grease. Figs. 2 (a) and (b) illustrate the axial and radial strain distributions in a fully drained test on a specimen contained between conventional frictional type ends. The specimen was isotropically consolidated to 60 psi. In these figures each line corresponds to the equilibrium strain distribution in the specimen at the end of each deviator stress increment. The results indicate both the axial and radial strains are smallest at the two ends of the specimen. Also, for each increment of stress, the maximum strain was observed approximately at one third of the height from the base. The axial strain distribution up to an average value of 4% was reasonably uniform; these strains correspond to a stress ratio of 0.4. The radial strains were everywhere small in this range of stress ratio. Beyond a stress ratio of 0.4 the axial and radial strains became non-uniform. This development of non-uniformity caused a localised region near the base to bulge. Figs. 3 (a) and (b) refer to a similar test to that discussed for

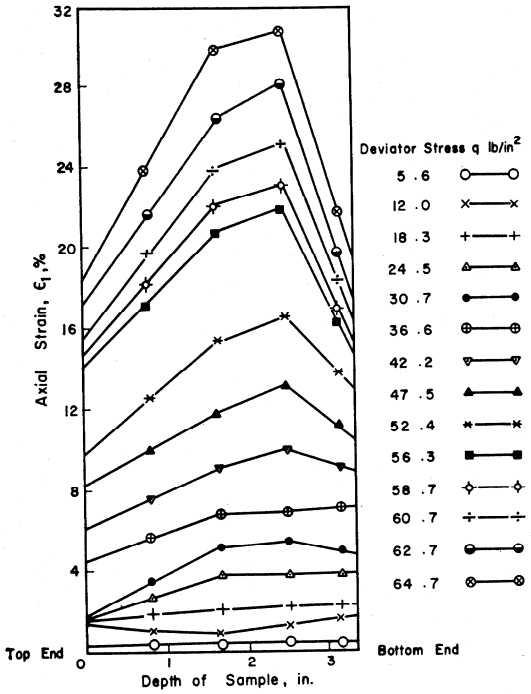

Fig. 2 (a). Axial strain distribution in sample contained between frictional ends

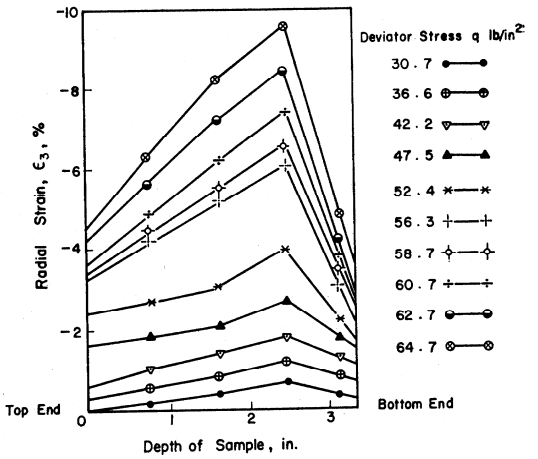

Fig. 2 (b). Radial strain distribution in sample contained between frictional ends

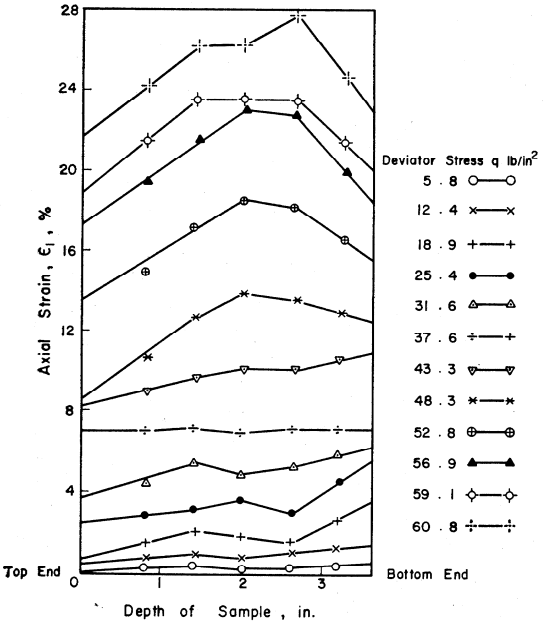

Fig. 3 (a). Axial strain distribution in sample contained between lubricated ends

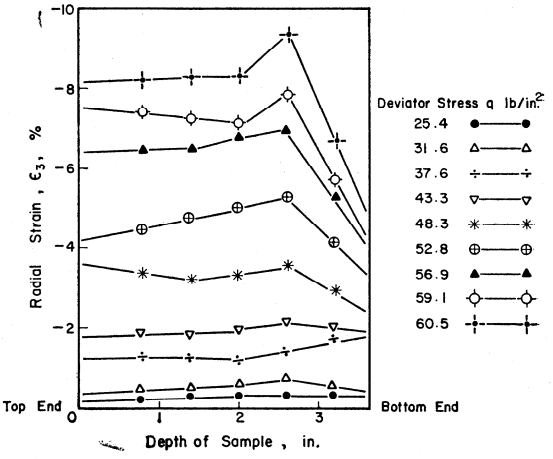

Fig. 3 (b). Radial strain distribution in sample contained between lubricated ends

Figs. 2 (a) and (b), but instead of conventional frictional ends the sample had the conventional lubricated ends. There is a marked improvement in the uniformity of the distribution of axial and radial strains in the sample with the lubricated end condition. The strains were reasonably uniform up to 9% overall axial strain. This strain corresponded to a stress ratio of 0.50 which was approximately 4/5 th the peak stress ratio. Moreover even at the peak stress ratio, the stributions of strains in the sample with the lubricated ends were far more uniform than the sample contained between the frictional ends.

Principal Axes of Local Strains

Two methods were adopted in the calculations of local strains. In one method, only the axial and radial strains (ε_y, ε_x respectively) were calculated and the distortional strains were assumed to be negligible. Hence ε_y and ε_x would correspond to the principal strains. In the second method, ε_x, ε_y and γ_{xy} (distortional strain) were calculated and then the principal strains were evaluated from them. The first method was originally used by Sirwan (1965) and will be referred to as the "Sirwan's Method". The second method will be referred to as "Author's Method". In Fig. 4 (a) the local incremental axial strains obtained from Sirwan's method and from the author's method are compared. These local incremental strains were all for an increment of stress ratio of 0.08 from a stress ratio of 0.28. The corresponding comparison for local radial strains is made in Fig. 4 (b). In both figures the lines are equally inclined to the abscissa and ordinate axes of each diagram. If the experimental points all lie on these lines then it follows that the local principal axes of strain are vertical and horizontal throughout the samples. This can be seen to be the case.

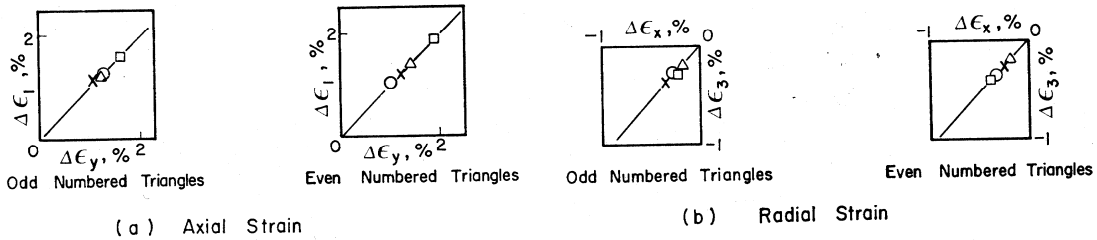

Fig. 4 (a). Comparison of local axial strains computed by two methods

Fig. 4 (b). Comparison of local radial strains computed by two methods

Comparison of the Overall Strains from the Average of Local Measurements and from the Boundary Measurements

Three tests *AX*, *AB* and *AQ* were performed each starting from an isotropic stress of 60 lb/in^2 and sheared along stress paths of slope (dq/dp) 1.5, 3 and α respectively. In these tests the overall axial and radial strains were obtained from the average of local measurements in both perpendicular planes in a sample, for each increment of stress ratio. From these strains the overall volumetric strains were computed at each stage of the test. The overall axial and volumetric strains were also computed from the measured changes in height and volume of the sample. These measurements will be referred to as the boundary measurement.

In Figs. 5 (a) and (b) the lines are equally inclined to the coordinate axes of the diagrams. Since the experimental points all lie on the lines it is evident that the strains computed from the boundary measurements are in agreement with the overall strains obtained by averaging the local measurements. The points in each figure correspond to the strains at the end of each increment, in a continuous test. The excellent agreement between the overall volumetric strains as obtained from the burette readings and as calculated from the lead shot displacements indicates that there was no leakage through the

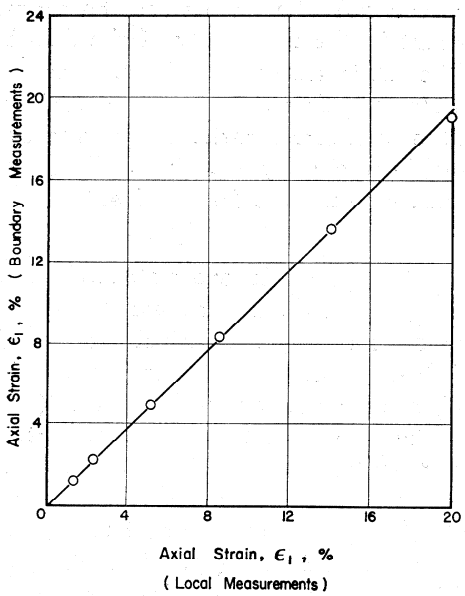

Fig. 5 (a). Comparison of average axial strains computed from local measurements and from boundary measurements

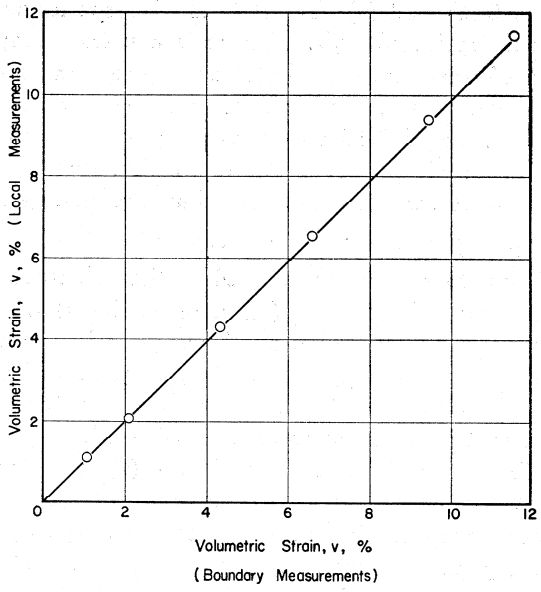

Fig. 5 (b). Comparison of average volumetric strains computed from local measurements and from boundary measurements

membrane ; the cell fluid was silicone oil. An extensive series of triaxial tests carried out by Ting (1968), indicated that the use of silicone oil as cell fluid virtually eliminates membrane leakage. Similar results were obtained for the samples AB and AQ which were sheared along stress paths of slope (dq/dp) 3 and ∞ respectively.

Displacement and Strain Patterns in a 4inch Diameter Sample of Normally Consolidated Kaolin during a Fully Drained Test

The lead shot markers were arranged within the sample in two mutually perpendicular planes. The markers in Plane 1 are shown in Fig. 6 and it contained, 6 columns (1-7), and 10 rows (A-J). Fig. 7 illustrates the vertical displacement of the markers plotted against the height of the markers above the base, for an increment in stress ratio $\Delta\eta=0.05$ from an initial stress ratio η of 0.5. It can be seen that for any one column of markers the vertical displacements are approximately linear with the heights of the markers indicating that the vertical strains are uniform throughout that column. Since the lines are parallel, the vertical strains in all columns are identical and hence the vertical strain is approximately uniform throughout the sample.

Fig. 8 gives the corresponding information for the horizontal displacements (when $\eta=0.5$ and $\Delta\eta=0.05$) plotted against the positions of the markers along the sample diameter. The observed data now lie only very approximately on straight lines and these are again parallel except for the rows A and J which were only 0.1 inch from the end platens. (When inspecting Fig. 8 it must be noted that the observed displacements correspond to local horizontal strains of magnitude 0.3%). The above incremental displacement patterns were typical of those obtained for each increment of stress ratio prior to the attainment of its peak value at which $0.65>\eta>0.55$. An attempt was made to determine the distribution of incremental displacements and strains during failure as defined by the maximum stress ratio η. When η was 0.55 the sample was stable and radiographs of planes 1 and 2 were taken. An increment $\Delta\eta=0.1$ was then applied and the ram of the triaxial cell

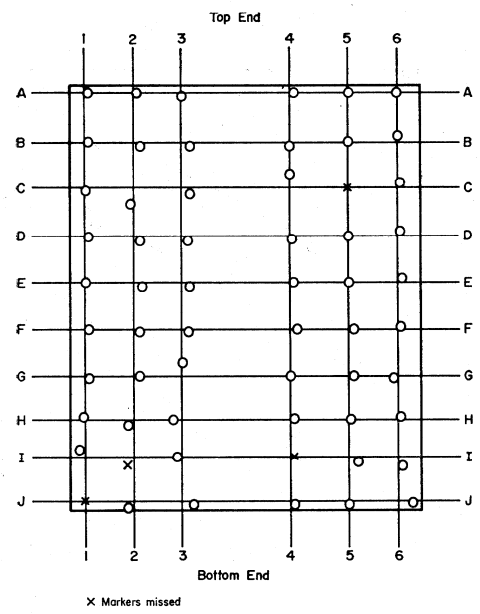

Fig. 6. Arrangement of lead markers in 4 inch diameter sample

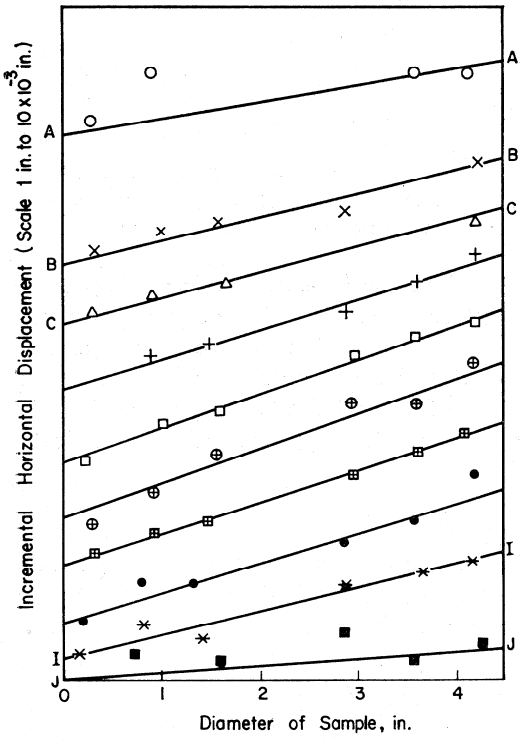

Fig. 8. Horizontal displacement of lead markers plotted with respect to the positions of the markers along the sample diameter

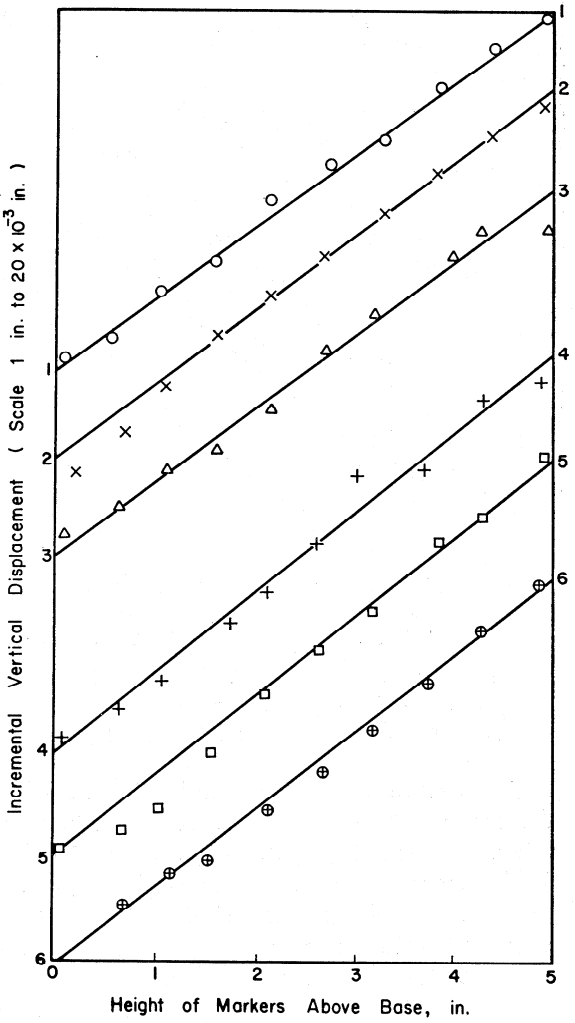

Fig. 7. Vertical displacement of lead markers plotted with respect to the height of the markers above base

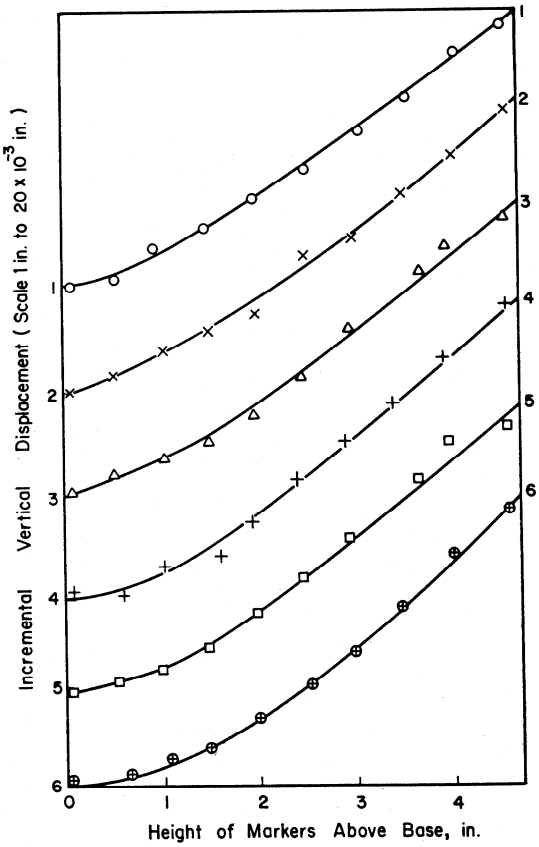

Fig. 9. Vertical displacement of lead markers plotted with respect to the height of the markers above base (at failure)

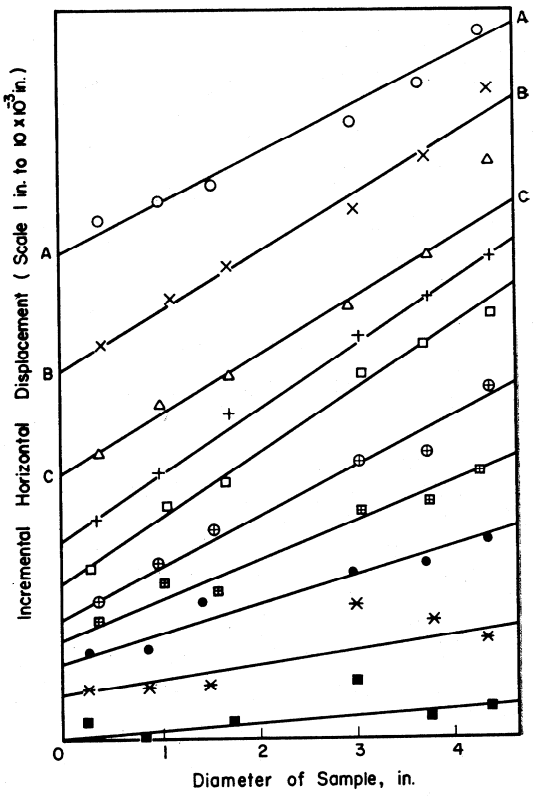

Fig. 10. Horizontal displacement of lead markers plotted with respect to the positions of the markers along the sample diameter

began to move slowly downwards with a small acceleration. At intervals during this process the ram was temporarily locked in position for about 15 minutes while radiographs were taken of Planes 1 and 2. Figs. 9 and 10 show typical distribution of local incremental displacements that occurred in an interval between successive radiographs in Plane 1. The patterns for Plane 2 were similar to those for Plane 1 for all the tests discussed in this paper and hence data will only be presented for Plane 1. The patterns clearly indicate that the strains were not uniform.

Extension Tests on Cylindrical Specimens of Kaolin

The internal displacement and strain patterns in a 1.5 inch diameter specimen sheared in extension will now be considered. The specimens were subjected to a maximum isotropic consolidation pressure of 60 lb/in^2 and subsequently sheared along a constant p stress path. The incremental vertical displacements of the markers for the first two increments of stress applied at stress ratios of, 0 and 0.42, were found to be linear with respect to the height of the sample. Beyond this stress level the displacement pattern is non-linear indicating that the strain is non-uniform. The corresponding incremental axial strain distributions are provided in Figs. 11 (i) to (iv). The strains were approximately uniform for the first two increments of stress. Marked non-uniformity was observed in the strain for the third

increment of stress and in the fourth there was gross non-uniformity. The radial strain distributions in Figs. 12 (i) to (iv) reveal similar phenomena to those observed for the axial strains.

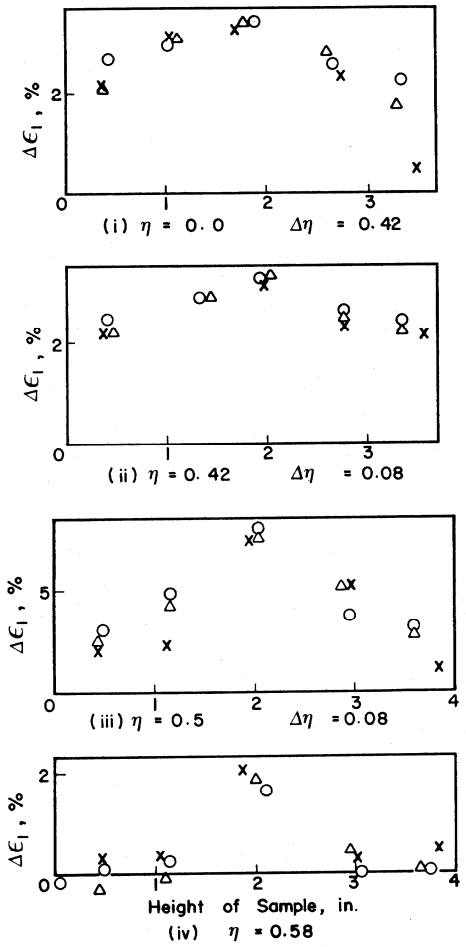

Fig. 11. Axial strain distribution in 1.5 inch diameter triaxial specimen sheared under extension conditions

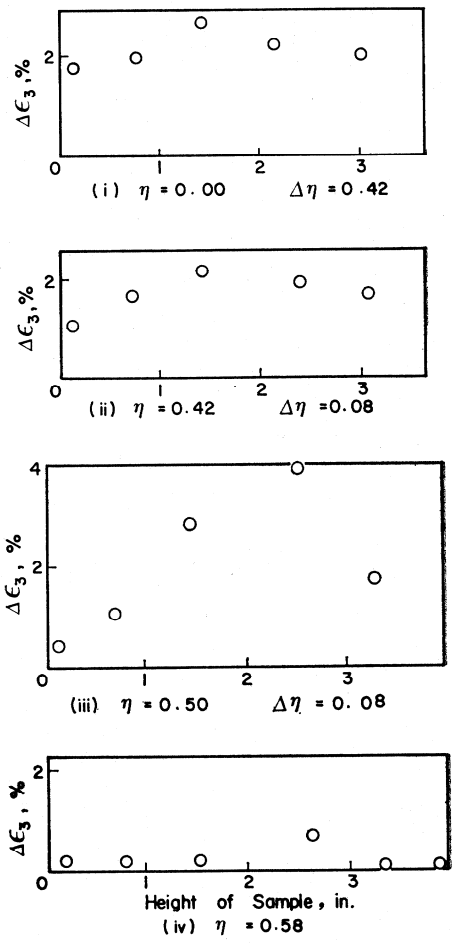

Fig. 12. Radial strain distribution in 1.5 inch diameter triaxial specimen sheared under extension condition

In contrast to their behaviour in compression tests, specimens in extension tests are more liable to develop local regions of high deformation. Photo. 2 shows photographs of radiographs taken during the compression test at five stages of strain of a heavily overconsolidated sample. Photo. 2 (v) corresponds to conditions after a failure plane has developed and well after the attainment of the peak stress ratio. Photo. 3 represents corresponding radiographs during the extension test discussed above. The onset of the development of the neck is clearly seen in Photo. 3 (iv) and its full development in (v). Between the interval of time corresponding to the two radiographs, all deformation has occurred in the 'necking' region. Close inspection of Photo. 3 shows the development of thin cracks just before and after the peak stress ratio condition was attained.

Deformation Characteristics During Failure in Compression and in Extension

The formation of rigid end zones during destructive tests in materials with low

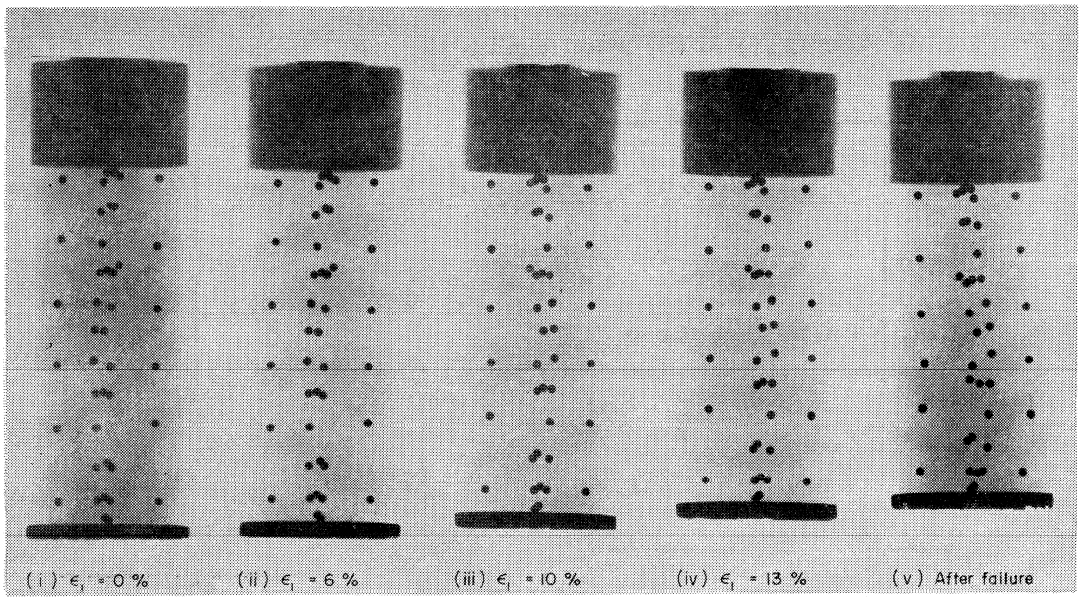

Photo. 2. Triaxial specimen at different stages of strain during a compression test

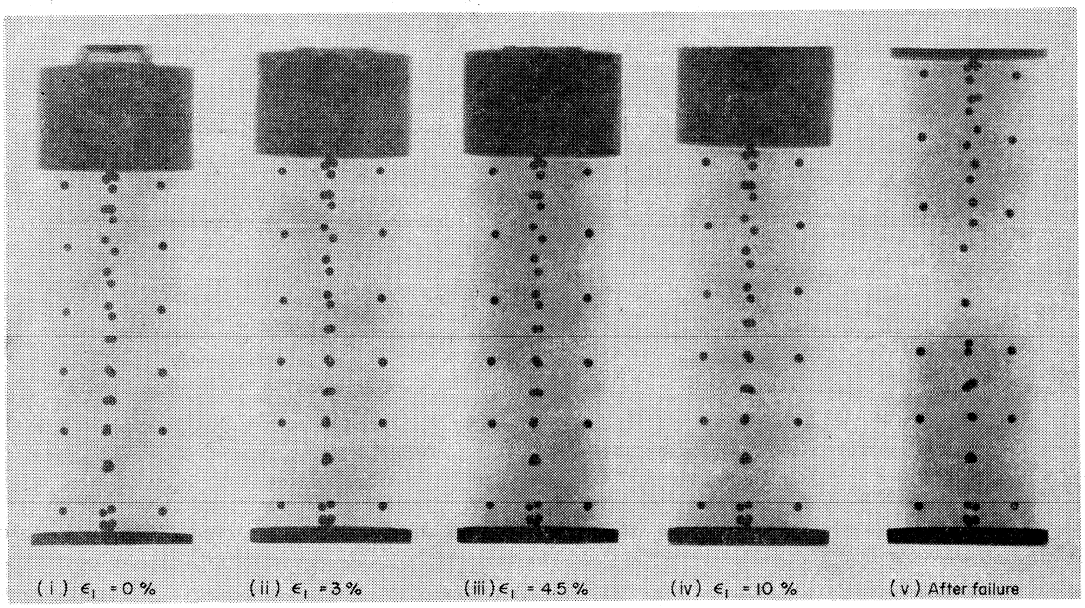

Photo. 3. Triaxial specimen at different stages of strain during an extension test

cohesion has been reported by several authors. These zones develop due to the end conditions and the lack of continuity and isotropy of the material tested. Zelenin and Lomise (1961) introduced coloured layers of soils and clay specimens and demonstrated the formation of such rigid end zones in their sample during deformation. By extending the theorem of Bishop, Green and Hill (1956), who states that "any region shown to be rigid for a particular stress field must be rigid in all complete solutions", Haythornthwaite (1960) isolated conical regions at the ends of the specimens as being rigid. He reported that this conical region subtends a semi-vertical angle of $(45-\phi/2)$ with the axis of the specimen.

For a value of ϕ of 20°, this angle will be 35°. The tests carried out by the Author on Kaolin had maximum stress ratios corresponding to $\phi = 20°$.

In Fig. 13, the mesh of continuous lines was made by connecting images of the lead shot markers on a radiograph taken of a given instant during the early stages of progressive failure of the sample. The dotted lines were obtained from the positions of the same markers in a subsequent radiograph which was taken after appreciable progressive failure had occurred. In Fig. 13 the shape of a mesh in the second radiograph is superposed on its shape in the first in such a way that the mesh has not rotated and the geometric centres of both meshes coincide. Consequently, while the full lines in Fig. 13 represents the initial shapes of the meshes, the dotted lines represent the shapes of the meshes after deformation. If the gap between neighbouring dotted lines is of uniform width round every mesh then the sample would have strained uniformly throughout. Where the gap is widest the greatest deformation will have occurred and where the dotted lines coincide with the full lines then no deformation would have taken place. In Fig. 13 when dotted lines do not appear they have coincided with the full lines. It can be seen that no deformations has occurred in the conical zones at the ends of the sample. The zones are therefore rigid, the mesh size of the lead shot network should have been reduced to specify them accurately. The conical zones are much smaller than those predicted by Haythornthwaite, since their semi-vertical angle is 59° compared to his predicted value of 35°, it is interesting to note that the angle

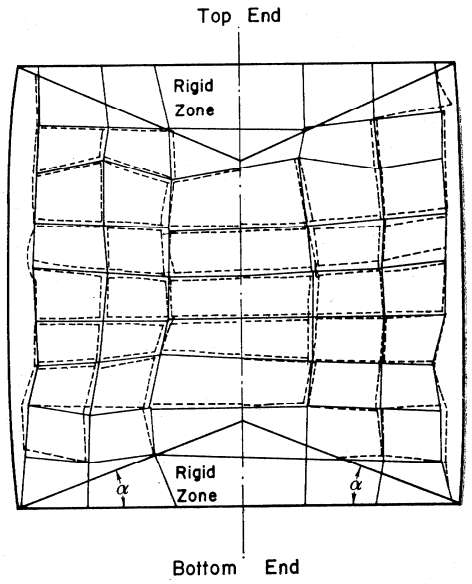

Fig. 13. Formations of conical rigid end zones during compression tests

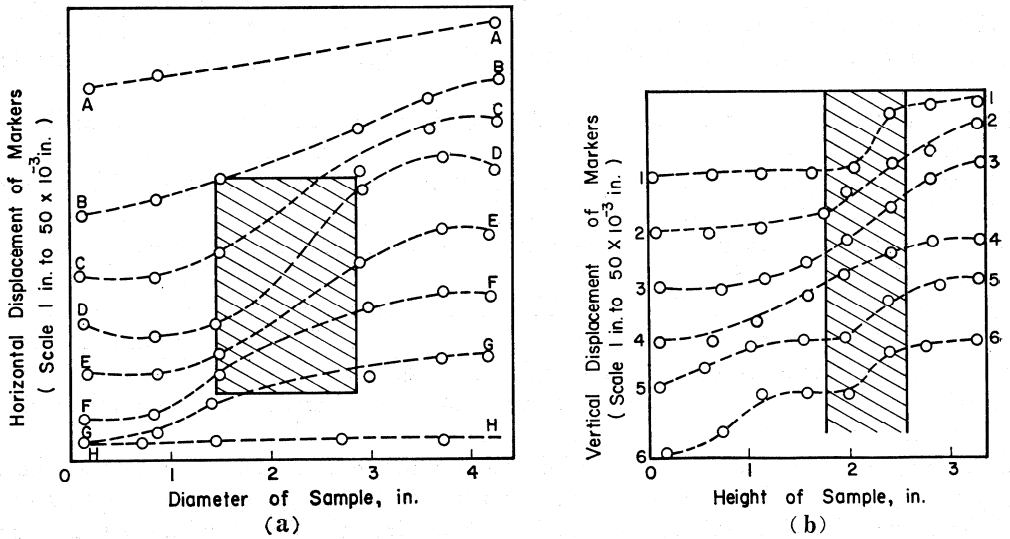

Fig. 14. Displacement patterns during failure showing central core with large deformation

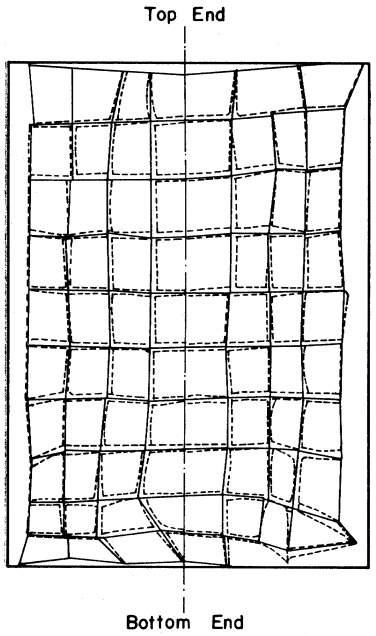

Fig. 15. Displacement pattern inside 4 inch diameter specimen failing in extension

α in Fig. 13 is 21° which is very close to the angle ϕ (=20°) for Kaolin. In Fig. 14 (a) the axial displacements were plotted against the heights of the markers above the sample base for all the six vertical columns in Plane 1. The bottom of the sample is to the left of this diagram so that in effect the sample is on its side. The axial strains which are proportional to the slopes of the dotted lines (with respect to the base of the diagram), can be seen to be the largest in the inner core of a horizontal layer in the sample represented by the shaded region in this diagram. In Fig. 14 (b) the corresponding information is given for the radial displacements of the markers in the horizontal rows AA, ···, HH, with respect to the position of the markers along the diameter. The slope of the dotted curve is a measure of the radial strain at that point. It can be seen that most of the radial strain is occurring in the central core shown shaded in Fig. 14 (b).

Fig. 15 illustrates the displacement pattern inside the 4 inch diameter specimen OE, while failing in extension and may be compared with the corresponding pattern in Fig. 13 for a specimen failing in compression. It is evident that for specimens failing in extension, there are no rigid zones forming at the ends of the specimen as those noted in the sample tested under compression conditions. The theoretical analysis of Haythornthwaite indicates rigid zones at the ends of the specimens even in extension. These rigid zones were reported by him to subtend an angle of $(45-\phi/2)$ with the base.

CONCLUSIONS

The effects of end restraint on the axial and radial strain distributions were determined for 1.5 inch diameter specimens contained between (i) frictional ends and (ii) lubricated ends, during a fully drained test. The strain distributions plotted for all increments of stress up to failure showed that

(i) marked non-uniformity in strain developed in the specimens contained between friction ends,

(ii) substantially uniform strains (up to about 75% of the peak stresses), for specimens contained between lubricated ends.

(iii) the principal axes of the local strains were coincident with the vertical and horizontal axes of the specimen, and,

(iv) the overall average axial and volumetric strains computed from the local strain measurements were in excellent agreement with the overall average measurements conventionally measured using a dial gauge and a burette.

The local measurements of strains carried out on 4.0 inch diameter sample revealed similar findings to that of the 1.5 inch diameter sample.

During progressive failure in compression, rigid zones were found to develop at the two ends of the specimens. These observed rigid zones were symmetrical about the axis of the sample and were found to subtend an angle of approximately $\phi=20°$ with the end plattens. Theoretical analysis carried out by Haythornthwaite for triaxial compression tests predicted

the formation of rigid zones, the boundaries of which subtend an angle with the end plattens of $(45+\phi/2)$. No rigid zones were observed during progressive failure in extension tests, though Haythornthwaite's analysis would predict the formation of rigid zones subtending an angle of $(45-\phi/2)$ with the base.

ACKNOWLEDGEMENTS

The experimental work presented in this paper was carried out in the Engineering Laboratories at the University of Cambridge. The author wishes to thank his supervisor Dr. R.G. James and the late Prof. K.H. Roscoe for their unstinted help and valuable guidance. The manuscript of this paper was prepared at the Asian Institute of Technology. Thanks are due to Prof. Za-Chieh Moh, Dr. Edward W. Brand and Mrs. Vatinee Chern.

NOTATION

p = mean normal stress
q = deviator stress
v = volumetric strain
x, y = Cartesian coordinates
σ_1', σ_2', σ_3' = principal effective compressive stresses
ε_1, ε_2, ε_3 = principal compressive strains
ε_y = strain in y-direction (vertical)
ε_x = strain in x-direction (horizontal)
γ_{xy} = distortional strains in xy plane
ε = deviator strain
Δ = denotes increments
ϕ = angle of internal friction
α = angle made by the rigid end zones of the triaxial sample with the end plates

REFERENCES

1) Balasubramaniam, A. S. (1974): "Local strains in cylindrical specimens of kaolin during consolidation," Geotechnical Engineering, Journal of Southeast Asian Society of Soil Engineering, Vol. 2, December.
2) Balla, A. (1960): "Stress conditions in triaxial compression," J. Soil Mech. Found. Div., A. S. C. E., Vol. 86, pp. 57-84.
3) Bishop, J. W., Green, A. P. and Hill, R. (1956): "A note on the deformable region in a rigid plastic body," J. Mech. Phys. Solids, Vol. 4.
4) Burland, J. B. and Roscoe, K. H. (1969): "Local strains and pore pressures in a normally consolidated clay layer during one dimensional consolidation," Geotechnique, Vol. 19, pp. 335-356.
5) D'Appolonia, E. and Newmark, N. M. (1951): "A method for the solution of the restrained cylinder under compression," Proc., 1st U. S. Nat. Cong. Appl. Mech., A. S. M. E., pp. 217-226.
6) Filon, L. N. G. (1902): "On the elastic equilibrium of circular cylinders under certain practical systems of load," Philosophical Transaction of the Royal Society, Vol. 198(A), pp. 147-223.
7) Geuze, E. C. W. A. and Tan, T. K. (1950): "The shearing properties of soils," Geotechnique, Vol. 2, No. 2, pp. 141-161.
8) Haythornthwaite, R. M. (1960): "Mechanics of the triaxial test for soils," J. Soil Mech. and Found. Eng., A. S. C. E., Vol. 86, pp. 35-62.
9) Pickett, G. (1944): "Application of the fourier method to the solution of certain boundary problems in the theory of elasticity," J. Appl. Mech., A. S. M. E., 11, A-176.
10) Roscoe, K. H., Authur, J. R. F. and James, R. G. (1963): "The determination of strains in soils by an X-ray method," Civ. Eng. and Pub. Wrks Rev., 58, pp. 873-876 and 1009-1012.
11) Roscoe, K. H., Schofield, A. N. and Thurairajah, A. (1963): "A critical appreciation of test data

for selecting a yield criterion for soils," Proc. Symposium on Laboratory Shear Testing of Soils, A. S. C. E. and N. R. C. C., pp. 111-128.
12) Roscoe, K. H., Schofield, A. N. and Wroth, C. P. (1958): "On the yielding of soils," Geotechnique, Vol. 8, pp, 22-53.
13) Rowe, P. W. and Barden, L. (1964): "The importance of free ends in the triaxial test," J. Soil Mech. and Found. Eng., A. S. C. E., Vol. 90, SM 1, pp. 1-27.
14) Schofield, A. N. and Wroth, C. P. (1968): Critical State Soil Mechanics, McGraw-Hill, London.
15) Shockley, W. G. and Ahlvin, R. G. (1960): "Non-uniform conditions in triaxial test specimens," Proc. Res. Conf. on Shear Strength of Cohesive Soils, A. S. C. E., pp. 341-357.
16) Sirwan, K. Z. (1965): "Deformation of soil specimens," Ph. D. Thesis, Cambridge University.
17) Ting, W. H. (1968): "Some effects of history on the stress-strain behaviour of kaolin," Ph. D. Thesis, Cambridge University.
18) Zelenin, A. N. and Lomize, G. M. (1961): "The compressive strength of soil samples in relation to the limited plastic soil deformation," Proc. 5th Int. Conf. Soil Mech. Found. Eng., Vol. 1, pp. 423-425.

(Received July 7, 1975)